FIRST LUNAR OCCURRENCE OF KEIVIITE-(Y) IN TROCTOLITIC ANORTHOSITE 76335.

P. Carpenter[1], J. Edmunson[2], B. A. Cohen[3], , R. A. Zeigler[1], and B. L. Jolliff[1], [1]Washington University, EPSC CB 1169, St. Louis MO 63130, paulc@levee.wustl.edu, [2]BAE Systems/Marshall Space Flight Center/VP33, Huntsville AL, [3]Marshall Space Flight Center/VP62.

Introduction: During routine electron-probe microanalysis (EPMA) and backscattered-electron (BSE) imaging of lunar troctolitic anorthosite 76335,59 section, a 3 x 10 μm yttrium silicate was identified and preliminary results summarized [1]. Based on EPMA analysis this mineral has been identified as keiviite-(Y) with the formula $(Y,REE)_2Si_2O_7$, and we report the first lunar occurrence of this phase which is known previously only in terrestrial occurrences. The REE concentrations of lunar keiviite-(Y) are distinct compared to reported terrestrial examples. The keiviite-(Y) is intimately in contact with a merrillite crystal which has a distinctive REE composition compared to other merrillites in 76335. The complex REE chemistry, small size of the lunar keiviite-(Y), and metamict nature of the phase required careful analysis using EPMA and related analysis tools, and a summary of the characterization is presented.

Terrestrial Keiviite and Yttrialite: The lunar keiviite-(Y) is similar to two terrestrial $(Y,REE)_2Si_2O_7$ sorosilicate minerals, yttrialite-(Y) and keiviite-(Y), which are named for the dominant REE and in which Y is replaced by REE (Table 1). Yttrialite-(Y) from Ivedal Norway is comparable but contains a significantly higher Th concentration [2]. Keiviite-(Y) exhibits solid solution with heavy REE (HREE) in keiviite-(Yb) but no extensive series of other HREE are documented. The lunar phase is more similar to keiviite-(Y) from the Kola peninsula of Russia, which occurs in quartz and fluorite vein-fill of amazonitic rand-pegmatites[3,4]. Y and HREE-rich phases are most well developed in rocks exhibiting extensive metasomatism at this locality. Keiviite is also observed as small inclusions in altered terrestrial zircons. Due to small crystal size and analytical complexity, few modern EPMA analyses have been published on terrestrial keiviite and yttrialite.

Analytical Methods: The lunar keiviite-(Y) crystal was analyzed on the Washington University EPS JEOL JXA-8200 Superprobe, and was studied using energy-dispersive (EDS) and wavelength-dispersive spectrometry (WDS), and Monte-Carlo simulation. WDS wavescans were used to confirm the element inventory and identify background positions for use in all REE standards and samples. EPMA was performed at 15 kV accelerating voltage and 40 nA probe current, and the primary L-family x-ray lines were measured using both LiF and LiFH diffracting crystals. REE single-crystal phosphate standards were used for primary calibration, x-ray peak overlap correction, and background locations; Pb-free regions were used for calibration [5,6]. A suite of secondary REE standards were used to confirm the accuracy of analysis (e.g., Drake and Weill REE glasses, University of Edinburgh REE-rich glasses and several REE trace element glasses) [7]. Counting times of 60-300 sec were used and three separate analytical runs were conducted to confirm accuracy within an individual run and the reproducibility of measurements made with a new standardization.

EPMA of REE phases is a challenge due to L-family x-ray peak interferences, spectral complexity and background selection, and (for small samples) sampling due to electron scattering and secondary x-ray fluorescence of the surrounding matrix. Probe for EPMA microprobe software was used for analysis and data correction [8]. The full list of REE was analyzed and all observed REE x-ray peak interference corrections were established. This interference correction is superior to historically used empirical overlap factors as the interference intensities are adjusted and corrected inside the ZAF iteration loop. Simultaneous WDS measurements using two spectrometers were made on all REE for both verification and improved counting statistics. The accuracy of background measurements was evaluated using WDS off-peak direct measurement, and was compared with a mean atomic number background empirical correction which utilized the primary calibration standards. This study is the first to perform a full analysis of all REE elements with a calibration that in principle can be used to analyze the full concentration range from trace level to major element concentrations, and represents a significant improvement in analytical capability.

The keiviite-(Y) crystal is in contact with a larger RE-merrillite crystal in a small cavity in the 76335 sample (figure 1). The preliminary analyses of keiviite-(Y) (see ref [1]) exhibit both Ca and P at much higher concentrations than observed in terrestrial keiviite. Monte Carlo simulation using DTSA-II software was used to simulate a 1.5 μm keiviite-(Y) crystal (using Ca and P-free lunar analysis) embedded in a RE-merrillite matrix. This simulation demonstrated that primary electron scattering extended through the keiviite into the merrillite, and x-rays generated in the excitation

volume produced secondary fluorescence of Ca and P x-rays in the RE-merrillite crystal (figure 2) [9]. The simulated and observed EDS spectra confirm that Ca and P were sampled from the RE-merrillite which justifies the recalculation of the keiviite-(Y) analysis to a Ca and P-free basis as a result.

The resulting formula for the lunar keiviite-(Y) is $(Y_{1.4}REE_{0.43}Mg_{0.09}Fe_{0.06}Pb_{0.01}Th_{0.01})Si_2O_7$ with a cation sum of 4.05. Figure 3 shows the REE patterns for the lunar keiviite-(Y) and is compared to the terrestrial yttrialite-(Y) and keiviite-(Y) data from Table 1, and to the adjacent RE-merrillite and a RE-merrillite from 7335,69.

Table 1: Mineral Analyses of yttrium silicates

Oxide	Kv 1	Yt 1	Kv 2	Kv 3
SiO_2	32.44	28.70	30.49	33.03
MgO	1.00	0.15		
CaO	(0)	0.93	0.00	0.27
Y_2O_3	42.46	31.37	45.86	57.92
La_2O_3	2.28	0.14		
Ce_2O_3	3.63	0.66		
Pr_2O_3	0.10	0.15		
Nd_2O_3	0.28	1.09		
Sm_2O_3	0.19	1.17		0.47
Gd_2O_3	0.69	2.44	0.62	0.78
Tb_2O_3	0.29	0.61	0.00	
Dy_2O_3	3.77	5.35	2.92	1.86
Ho_2O_3	1.07	1.00	1.27	0.70
Er_2O_3	4.78	3.69	4.40	2.42
Tm_2O_3	0.68	0.75	1.11	0.34
Yb_2O_3	2.81	5.58	11.81	1.24
Lu_2O_3	0.39	1.45	1.05	0.06
Total	(100)	100.18	99.83	99.09

Kv1. Lunar keiviite-(Y) from 76335,59 troctolitic anorthosite. Normalized on Ca and P-free basis. Includes 0.24 TiO_2, 1.13 FeO, 0.77 PbO, 0.83 ThO_2, 0.04 UO_2
Yt1. Yttrialite-(Y), Ivedal Norway. Includes 1.18 Fe_2O_3, 0.48 MnO, 6.97 ThO_2, 2.59 UO_2, 3.68 H_2O
Kv2. Keiviite-(Y), Mt. Ploskaya, Kola Peninsula, Russia
Kv3. Keiviite-(Y), amazonitic rand pegmatite, Kola Peninsula, Russia
Elements not detected are not listed. All values in oxide weight percent

Discussion: Keiviite-(Y) is formed in terrestrial environments with high Y activity and availability of Si in pegmatitic and metasomatic processes. The occurrence of lunar keiviite-(Y) at the lithologic boundary between orthopyroxene and olivine-dominated assemblages, in what appears to be a void with associated merrillite, suggests that metasomatic processes and possible vapor-phase deposition are important. The improved capability of modern electron-microprobe software and analysis tools makes the quantitative analysis of the keiviite-(Y) possible. Because the crystal is small and metamict it is not possible to perform other analytical techniques, but the identification as keiviite-(Y) is straightforward in this case.

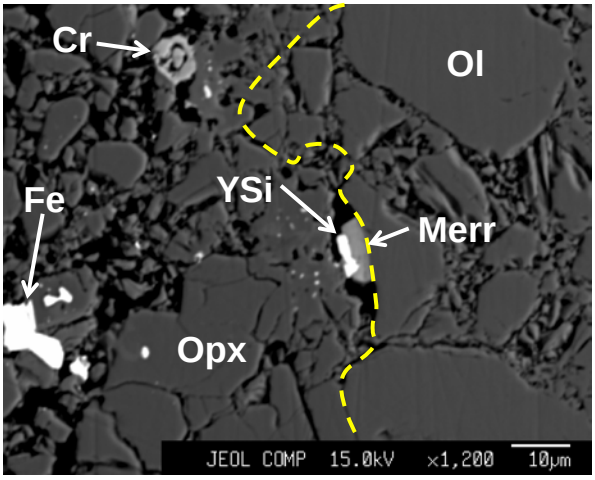

Figure 1: BSE image of keiviite-(Y) (YSi) and RE-merrillite (Merr) in lunar troctolite 76335,59. Yellow dashed line indicates approximate location of orthopyroxene/olivine border. Ol = olivine, Opx = orthopyroxene, Cr = chromite, and Fe = native iron-nickel metal.

Figure 2: EDS spectra of 76335,59 keiviite-(Y) in blue compared to DTSA-II simulated EDS spectrum of 1.5 μm keiviite-(Y) inclusion in RE-merrillite matrix.

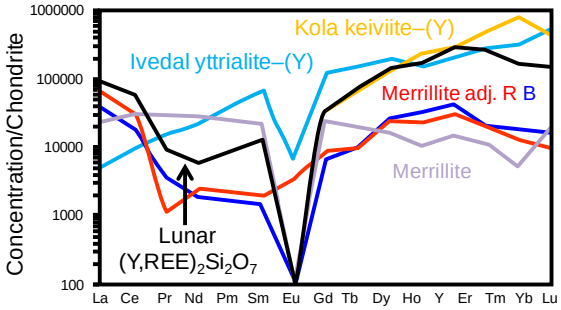

Figure 3: REE patterns for 76335,59 keiviite-(Y), RE-merrillite, and terrestrial yttrialite-(Y) and keiviite-(Y).

References: [1] Edmunson J. et al. (2010) *LPS XXXXI*, 2627. [2] Nilssen, B. (1971) Norsk. Geol. Tidsskr., 51, 1-8. [3] Voloshin A.V. et al. (1985) Mineral. Zhurnal 7(6), 79-94. [4] Jones A.P. et al. (1996) Rare Earth Minerals, Chapman and Hall, Ch 12. [5] Donovan J. et al. (2003) Can. Mineral.41,221-232. [6]Smithsonian Microbeam Standards [7] Drake M.J. and D.F. Weill (1971) Chem. Geol. 10, 179-181. [8] Probe Software Inc. [9] NIST DTSA-II